CROSSOVER BETWEEN FERROELECTRIC ORDER AND DIPOLAR GLASS DISORDER IN BETAINE PHOSPHATE$_{0.06}$ BETAINE PHOSPHITE$_{0.94}$ MIXED CRYSTALS

J. Banys [a], J. Macutkevic [b], C. Klimm [c], and G. Völkel [c]

[a] *Vilnius University, Saulėtekio 9, LT-10222 Vilnius, Lithuania*
[b] *Center for Physical Sciences and Technology, A. Goštauto 11, LT-01108 Vilnius, Lithuania*
[c] *Fakultät für Physik und Geowissenschaften, Universität Leipzig, Linnestr. 5, D-04103 Leipzig, Germany*
E-mail: jan.macutkevic@gmail.com

The dielectric properties of mixed betaine phosphate$_{0.06}$ betaine phosphite$_{0.94}$ (BP$_{0.06}$BPI$_{0.94}$) ferroelectric crystals were investigated in a wide frequency range from 20 Hz to 3 GHz. Although the dielectric anomaly is clearly observed close to the ferroelectric phase transition temperature T_c = 121 K, the dielectric dispersion is very broad around and below this temperature. Temperature dependences of the dielectric strength, the mean relaxation frequency and the spontaneous polarization cannot be described together according to the Landau theory for ferroelectric phase transition with a single order parameter or according to the quasi-one-dimensional Ising model. The polarization shows a pronounced distribution in the ferroelectric phase and only a partial ordering of hydrogen atoms occurs down to the lowest temperatures. The unordered hydrogen atoms form a glassy phase and its formation is observed in dielectric spectra at very low temperatures. The proton freezing temperature was estimated.

Keywords: dielectric permittivity, ferroelectrics, distribution of relaxation times

PACS: 77.22.Gm, 02.30.Rz, 64.70.Pf, 77.84.Fa

1. Introduction

Nowadays, ordered systems with ferroelectric, antiferroelectric or (and) multiferroic properties are very popular due to their outstanding dielectric, piezoelectric, piroelectric and other properties [1]. In order to control these properties, the doping or the substitutions are often used. However, too big amount of impurities can smear out the ferroelectric properties. Various ferroelectric phase smearing scenarios are possible, for example, the dipolar glass phase or the nonergodic relaxor phase can appear in doped materials at low temperatures [2]. Therefore, investigations of disordered systems with relaxor, dipolar glass or other properties are also very important [3].

Betaine phosphate (BP) (CH$_3$)$_3$NCH$_2$COOH$_3$PO$_4$ and betaine phosphite (BPI) (CH$_3$)$_3$NCH$_2$COOH$_3$PO$_3$ are crystals consisting of amino acid betaine as an organic, and phosphoric and phosphorous acids, respectively, as an inorganic component. The structure of both compounds is very similar [4–6]. The PO$_4$ or, respectively, PO$_3$ groups are connected by hydrogen bonds and form quasi-one-dimensional chains along

the monoclinic *b* axis [4]. The betaine molecules are arranged almost perpendicular to this chain along the *a* direction and are linked by one (BPI) or two (BP) hydrogen bonds to the inorganic group [4]. The antiferrodistorsive phase transition is observed in BPI at 355 K and in BP at 365 K (the symmetry change is $P2_1/m \rightarrow P2_1/c$) [4, 6]. At higher temperatures the PO$_4$ or HPO$_3$ groups and the betaine molecules are disordered. They both order in the antiferrodistortive phase, but the hydrogen atoms linking PO$_4$ or HPO$_3$ groups remain disordered [5].

Ordering of these hydrogen atoms is a physical origin of the ferroelectric or the antiferroelectric phase transition, respectively. The ferroelectric phase transition was observed in BPI at 220 K (the symmetry change at the phase transition is $P2_1/c \rightarrow P2_1$) [5]. At low temperatures in BP two phase transitions were observed: the ferroelectric transition at 86 K (the symmetry change at the phase transition is $P2_1/c \rightarrow P2_1$) and the antiferroelectric phase transition at 81 K (the microscopic origin is related with a doubling of the unit cell along the *a* direction) [4]. The temperature dependence of the static dielectric permittivity of both

crystals fits very well a quasi-one-dimensional Ising model. So, the coupling between the dipoles within the chains is much stronger than that one between the dipoles in neighboring chains [4, 7]. Antiferroelectric order is established in BP at T_c = 81 K [8] in such a way that the O–H⋯O bonds order ferroelectrically within the one-dimensional chains whereas neighbouring chains are linked antiferroelectrically [5]. In BPI, however, neighbouring chains are linked ferroelectrically below T_c = 216 K [9]. Deuteration of hydrogen-bonded ferroelectrics leads to significant changes of the physical properties and shifts the temperatures of dielectric anomalies to the higher values [5]. For example, the ferroelectric phase transition in DBPI was observed at 297 K [9]. Only the antiferroelectric phase transition was observed in deuterated BP (DBP) at 119 K [10]. Therefore, the hydrogen bonds are very important for phase transitions in BP and BPI crystals at low temperatures.

According to the dielectric investigations of BPI, the dielectric dispersion in microwave frequency range close to the ferroelectric phase transition temperature fits the Debye equation and the relaxation frequency is a linear function of the temperature in the paraelectric phase [11]. At lower frequencies (below 1 GHz) in BPI an additional dielectric dispersion was observed, which is obviously related with dynamics of ferroelectric domains [11]. Close to the ferroelectric phase transition, the spontaneous polarization was observed in BPI [12]. A similar behaviour of dielectric dispersion was observed in BP crystals [13]. There the Debye model is also valid and the relaxation frequency has a minimum close to the ferroelectric phase transition temperature.

The BP_xBPI_{1-x} system was extensively studied experimentally [14–17] and theoretically [18, 19]. It is established that the low-temperature part of the (T, x) phase diagram of the BP_xBPI_{1-x} system consists mainly of (i) the ferroelectric phase for $0 \le x \le 0.1$, (ii) the antiferroelectric phase for $0.65 \le x \le 1$, and (iii) the so-called glass phase for $0.1 \le x \le 0.65$.

The main difference between the nondeuterated BP_xBPI_{1-x} and deuterated DBP_xDBPI_{1-x} systems is the highest temperatures of the dielectric anomalies in deuterated crystals. Both compounds show an abrupt decrease in T_c at small x with ferroelectricity completely destroyed at $x > 0.1$. The increase in T_c when hydrogen in hydrogen bonded ferroelectrics is replaced by deuterium was described theoretically [18].

Although a lot of investigations were performed for the mixed betaine phosphate–betaine phopshite crystals with the ferroelectric or the dipolar glass properties, the phase boundary between the ferroelectric and dipolar phase, i. e. mixed crystals with

$x \approx 0.1$, has not been investigated up to now. The aim of this work is to investigate dielectric properties of $BP_{0.06}BPI_{0.94}$ in a wide frequency range. We will demonstrate that the ferroelectric phase transition in $BP_{0.06}BPI_{0.94}$ is complex: the order and the disorder coexist in these crystals in a wide temperature range.

2. Experiment

$BP_{0.06}BPI_{0.94}$ crystals were grown by a controlled evaporation method from H_2O solution containing betaine with 94% phosphorous acid (H_4PO_4) and 6% phosphoric acid (H_3PO_3). More details about the growth of BP_xBPI_{1-x} crystals are in [16]. The single crystals were oriented along the monoclinic *b* axis. The complex dielectric permittivity $\varepsilon^* = \varepsilon' - i\varepsilon''$ was measured using the HP4284A capacitance bridge in the frequency range 20 Hz to 1 MHz. In the frequency region from 1 MHz to 3 GHz measurements were performed by a coaxial dielectric spectrometer with a vector network analyzer Agilent 8714ET. All measurements were performed on cooling with the controlled temperature rate of 0.25 K/min. Gold was used for contacting. Typical dimensions of the samples were ≈10 mm² area and ≈0.5 mm thickness.

3. Results and discussion

Temperature dependences of the complex dielectric permittivity $\varepsilon^* = \varepsilon' - i\varepsilon''$ of $BP_{0.06}BPI_{0.94}$ crystals at several frequencies in the ferroelectric phase transition region are shown in Fig. 1. At low frequencies (below 24 MHz) the position of dielectric permittivity maximum is frequency independent, indicating the ferroelectric phase transition temperature T_c = 121 K. There is a strong dielectric dispersion around and below the ferroelectric phase transition temperature T_c in the wide frequency range. At higher frequencies (above 24 MHz) the temperature of dielectric permittivity maximum T_m strongly increases with increasing frequencies.

The experimental data were described with the Cole–Cole formula:

$$\varepsilon^* = \varepsilon_\infty + \frac{\Delta\varepsilon}{1+(i\omega\tau_{CC})^{1-\alpha}}, \tag{1}$$

where $\Delta\varepsilon$ is the dielectric strength, τ_{CC} is the mean and most probable Cole–Cole relaxation time, ε_∞ is the contribution of phonon modes and electronic polarization to the static dielectric permittivity, and α is the parameter of the Cole–Cole distribution of relaxation times. The Cole–Cole parameters of ferroelectric dispersion are presented in Fig. 3. Only the parameter ε_∞
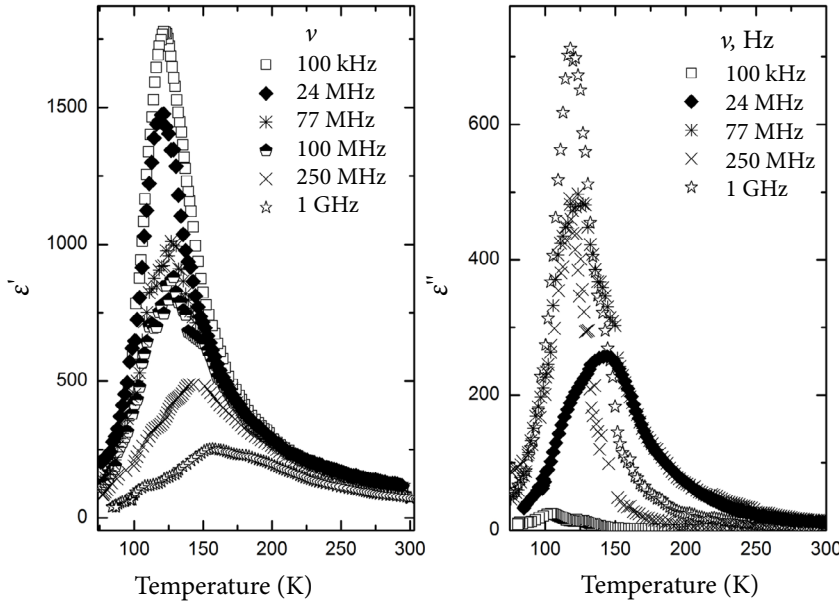
Fig. 1. Temperature dependence of complex dielectric permittivity for $BP_{0.06}BPI_{0.94}$ crystals (ferroelectric phase transition region).

does not vary with temperature. The dielectric dispersion looks like the Debye type dispersion only at higher temperatures ($T \gg T_c$). On cooling the parameter of distribution of relaxation times α of all investigated ferroelectrics increased. The extremely high value for ferroelectrics $\alpha = 0.3$ is observed at $T < T_c$ that displays the extremely broad distribution of relaxation times. This clearly differs from the monodispersive character, observed in BPI [13] ($\alpha_{max} = 0.04$), DBPI [20] ($\alpha_{max} = 0.12$) and $DBP_{0.01}DBPI_{0.99}$ ($\alpha_{max} = 0.2$) [21], while α deviates from its zero value only near T_C. The temperature dependence of the relaxation frequency $\nu_r = 1/(2\pi\tau_{CC})$ shows a minimum, this indicating the critical slowing down in the presented crystal. Such non-typical (for ferroelectrics) and not so easy-to-understand behaviour of distribution width α shows

that the Cole–Cole formula is not suitable for dielectric dispersion below T_c in the presented crystals (for enough high α and usual mean τ_{CC} the shortest relaxation times of Cole–Cole distribution of relaxation times lose their physical meaning).

The quasi-one-dimensional Ising model was used to fit the dielectric strength of ferroelectric dispersion [14]:

$$\Delta\varepsilon = \frac{C}{T}\left[\exp\left(-\frac{2J_{\parallel}}{k_B T}\right) - \frac{J_{\perp}}{k_B T}\right]^{-1}, \qquad (2)$$

where $J_{\parallel}$ and $J_{\perp}$ are the nearest neighbour intrachain and the effective mean field interchain coupling constants. The parameters obtained from the best fit
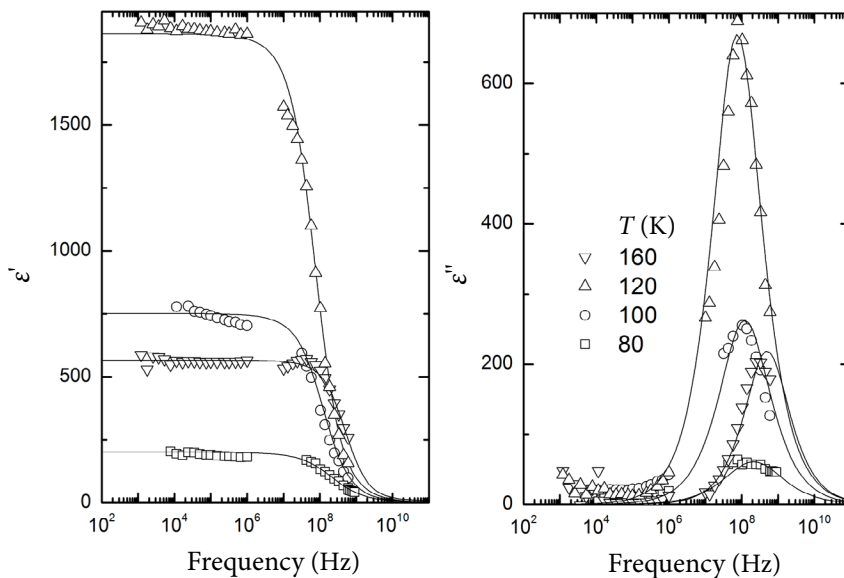

Fig. 2. Frequency dependence of complex dielectric permittivity for $BP_{0.06}BPI_{0.94}$ crystals. The solid lines are the best fit according to Eq. 4.
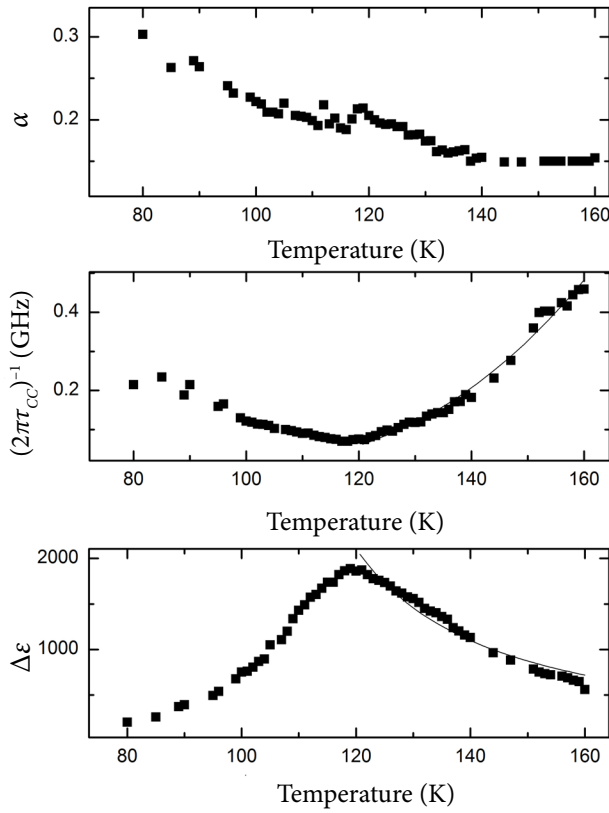
Fig. 3. Cole–Cole parameters for $BP_{0.06}BPI_{0.94}$ crystals.

(the solid line in Fig. 3) are $C = 28296$ K, $J_\perp/k_B = 15$, $J_\parallel/k_B = 86$ K and $J_\parallel/J_\perp = 5.73$.

The temperature dependence of the relaxation frequency shows a curvature in the high temperature phase (Fig. 3). The temperature dependence of the relaxation frequency according to the quasi one-dimensional Ising model [11] is given by

$$v_r = v_\infty \exp\left(-\frac{\Delta U}{k_B T}\right) \left[\cosh\left(\frac{2J_\parallel}{k_B T}\right)\right]^{-1}$$
$$\times \left[\exp\left(-\frac{2J_\parallel}{k_B T}\right) - \frac{J_\perp}{k_B T}\right], \tag{3}$$

where ΔU is the activation energy for the reorientation of the dipole, and v_∞ is the attempt frequency. Using the parameters $J_\parallel$ and $J_\perp$ obtained by means of Eq. (2), the best fit according to Eq. (3) results in the values $v_\infty = 0.65$ THz, $\Delta U/k_B = 481$ K.

The distribution of relaxation times $f(\tau)$ has been calculated directly from dielectric spectra according to the formulas

$$\varepsilon'(v) = \varepsilon_\infty + \Delta\varepsilon \int_{-\infty}^{\infty} \frac{f(\tau)\,d\lg\tau}{1+(\omega\tau)^2}, \tag{4a}$$

$$\varepsilon''(v) = \Delta\varepsilon \int_{-\infty}^{\infty} \omega\tau \frac{f(\tau)\,d\lg\tau}{1+(\omega\tau)^2}. \tag{4b}$$

The value of the Tichonov regularization parameter $\alpha_{Tch} = 4$ was determined as optimal. The distributions of relaxation times of the investigated ferroelectrics are presented in Fig. 4. In the ferroelectric phase the non-symmetric distribution of relaxation times has been obtained.
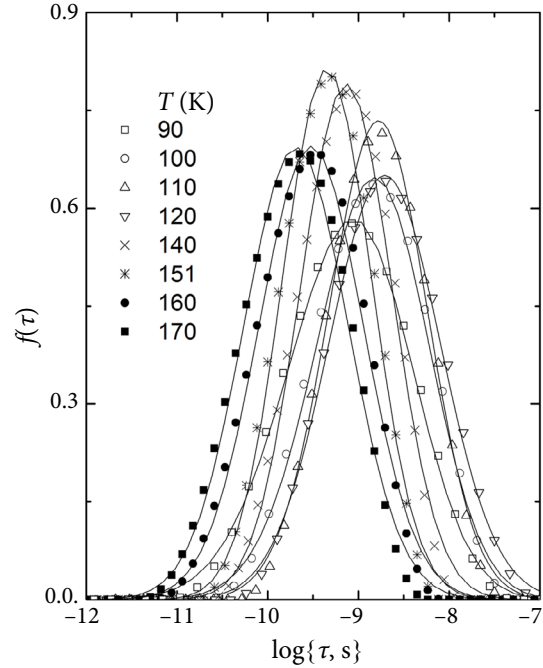

Fig. 4. Distributions of relaxation times for $BP_{0.06}BPI_{0.94}$ crystals.

We consider proton moving in the asymmetric double-well potential. The movement consists of fast oscillations in one of the minima with occasional thermally activated jumps between the minima. Here we neglect quantum tunneling, which is significant for protons at low temperatures. The jump probability is governed by the Boltzmann probability of overcoming the potential barrier between the minima. It was shown that the relaxation time of an individual hydrogen bond dipole in such [22] a system is given by

$$\tau = \tau_0 \frac{\exp[E_b/k_B(T-T_0)]}{2\cosh(A/2k_B T)}. \tag{5}$$

This equation is similar to the Vogel–Fulcher one, except the dominator, which accounts for the asymmetry A of the local potential produced by the mean field influence of all the other dipoles. Thus, the local polarization p (time-averaged dipole moment) of an

individual O–H⋯O bond is given by the asymmetry parameter A [22]:

$$p = \tanh(A/2k_B T). \tag{6}$$

We further consider that the asymmetry A and the potential barrier E_b of the local potential of the O–H⋯O bonds both are randomly distributed around their mean values A_0 and E_{b0} according to the Gaussian law resulting in the distribution functions:

$$f(E_b) = \frac{1}{\sqrt{2\pi}\sigma_{Eb}} \exp\left[-\frac{(E_b - E_{b0})^2}{2\sigma_{Eb}^2}\right], \tag{7}$$

$$f(A) = \frac{1}{\sqrt{2\pi}\sigma_A} \exp\left[-\frac{(A - A_0)^2}{2\sigma_A^2}\right], \tag{8}$$

where σ_{Eb} and σ_A are the standard deviations of E_b and A, respectively, from their mean values.

The distribution function of relaxation times is then given by

$$f(\ln \tau) = \int_{-\infty}^{\infty} f(A) f[E_b(A,\tau)] \frac{\partial E_b}{\partial(\ln \tau)} dA, \tag{9}$$

where $E_b(A,\tau)$ is the dependence of E_b on A for a given τ, derived from Eqs. (7) and (8).

Fits with the experimentally obtained relaxation-time distributions were performed simultaneously for seven different temperatures using the same parameter set: $\tau_0 = 4.32 \cdot 10^{-12}$ s and $T_{01} = 0$ K (as it should be for the ferroelectric phase transition). The results are presented in Fig. 4 as solid lines. The average local potential asymmetry A_0, the average potential barrier E_{b0} and the standard deviations σ_A and σ_{Eb} are temperature dependent as demonstrated in Fig. 5. At higher temperatures ($T \gg T_c$) the average local potential asymmetry A_0 and the standard deviation of asymmetry σ_A are small ($A/k_B = 37$ K and $\sigma_A/k_B = 0.9$ K for $T = 153$ K). In the ferroelectric phase on cooling the average asymmetry A_0 and the standard deviation σ_A strongly increased. However, in the presented ferroelectrics the average asymmetry A_0 is strongly higher than the standard deviation σ_A. In the paraelectric phase on cooling the average potential barrier E_{b0} increases and the standard deviation σ_{Eb} decreases, strongly correlating with the curvature of temperature dependence of the mean Cole–Cole relaxation time and the application of quasi-one-dimensional Ising models. The temperature dependence of the average potential barrier E_{b0} has a maximum at T_c, strongly correlating with slowdown of phase transition dynamics.

The spontaneous polarization of BP$_x$BPI$_{1-x}$ mixed crystals was investigated previously by the pyroelectric method [14]. Different approaches can be used to describe the temperature behaviour of the spontaneous polarization of ferroelectrics. According to the Ising model [12]

$$\langle \sigma_{sp} \rangle = \frac{\sinh \dfrac{J_\perp \langle \sigma_{sp} \rangle}{k_B T}}{\left[\sinh^2 \dfrac{J_\perp \langle \sigma_{sp} \rangle}{k_B T} + \exp\left(-\dfrac{4J_\parallel}{k_B T}\right)\right]^{1/2}}. \tag{10}$$

Moreover, according to this model the transition temperature $T_{C\,Ising}$ is determined by the condition

$$k_B T_{C\,Ising} \exp\left(-\frac{2J_\parallel}{k_B T_{C\,Ising}}\right) = J_\perp. \tag{11}$$
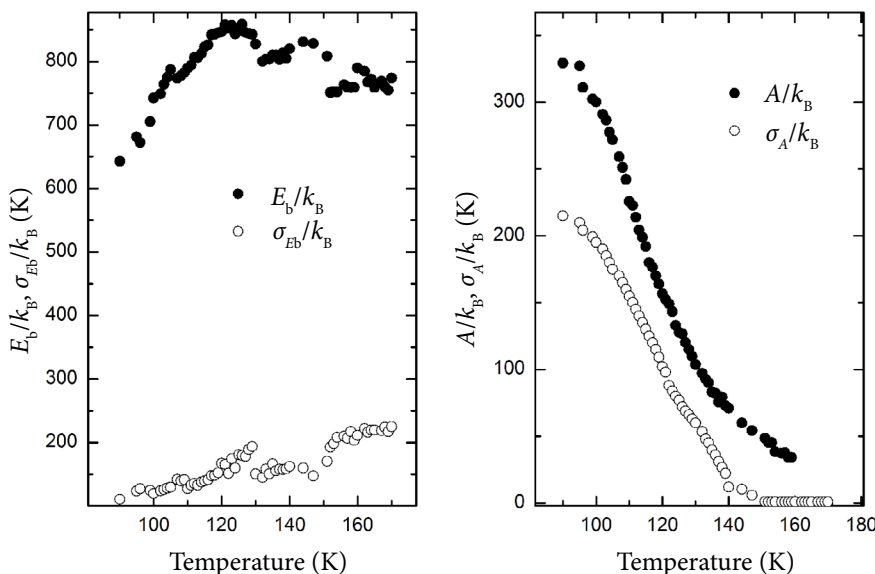

Fig. 5. Temperature dependence of double-well potential parameters for BP$_{0.06}$BPI$_{0.94}$ crystals.

The obtained transition temperature is $T_{C\,Ising} = 94$ K. Thus, we cannot describe with the Ising model formulas all the dependences together: $P(T)$, $\Delta\varepsilon(T)$ and $v(T)$, because the mismatch between $T_C - T_{C\,Ising}$ is significant. This becomes understandable from the below presented experimental results that the spontaneous polarization shows a remarkable distribution. The quasi-one-dimensional Ising model presupposes homogeneity [12] and cannot describe the non-homogeneous ferroelectrics. However, in nature crystals (including ferroelectrics and the same "pure" betaine phosphite) without impurities do not exist. A fundamental query is that at which concentration of impurities the discrepancy from the quasi-one-dimensional Ising behaviour becomes significant and essential. In the case of betaine phosphate the answer is 6%.

From the distribution function $w(A)$ of the local potential asymmetry the distribution function $w(p)$ of the local polarization of the hydrogen bonds can be deduced:

$$w(p) = \frac{2k_B T}{\sqrt{2\pi}\sigma_A (1-p^2)}$$
$$\times \exp[-\frac{[a\tanh(\mathrm{p}) - a\tanh(p_0)]}{2\sigma_A^2/(2k_B T)^2},$$

(12)

which transforms in the form known for the RBRF [23] model when substituting

$$\sigma_A = 2J\sqrt{q_{EA} + \Delta f},$$

(13)

and

$$A_0 = 2\Delta J\overline{p},$$

(14)

where $\overline{p}$ is the average polarization, J is the mean coupling and ΔJ is the rms variance of the coupling. The calculated distribution functions $w(p)$ of the local polarization are presented in Fig. 6(b). As we can see, they behave exactly as expected for an inhomogeneous ferroelectric [24].

Knowing the distribution function $w(p)$, both the average (macroscopic) polarization

$$\overline{p} = \int_{-1}^{1} pw(p)\mathrm{d}p,$$

(15)

and the Edwards–Anderson glass order parameter

$$q_{EA} = \int_{-1}^{1} p^2 w(p)\,\mathrm{d}p$$

(16)

can be calculated. The calculated average polarization values are presented in Fig. 6(a). As can be seen, the calculated average polarization is the best fit for ex-
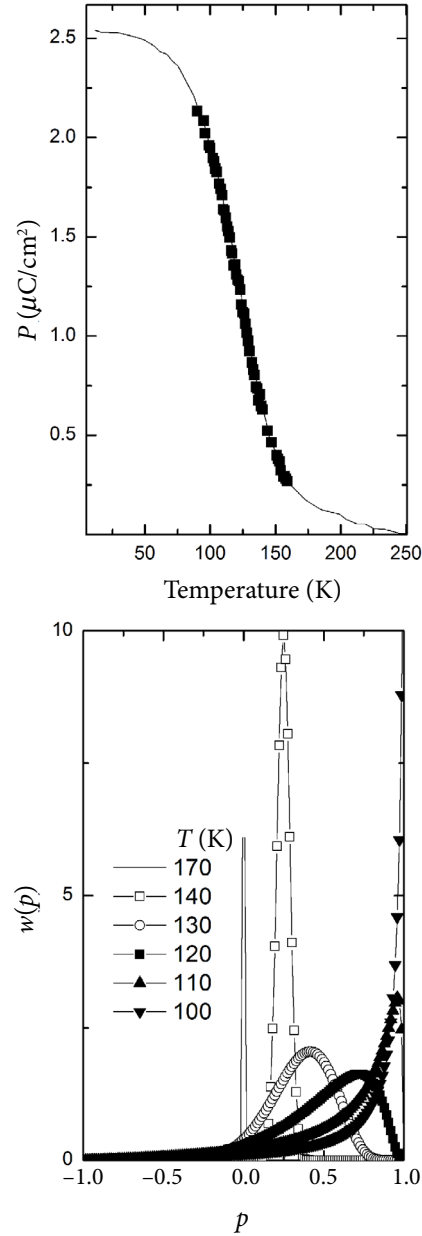

Fig. 6. Temperature dependence of the spontaneous polarization (a) (points are calculated according to Eqs. (12) and (15), the line is taken from [16]) and the distributions of the local polarization (b) for $BP_{0.06}BPI_{0.94}$ crystals.

perimental results presented in [14]. We can conclude that the extraction of continuous relaxation time distribution directly from the broadband dielectric spectra allows observing the distribution of local polarization inside ferroelectrics.

The dielectric dispersion does not vanish below the ferroelectric phase transition temperature (Fig. 7). The dielectric dispersion at very low temperatures has been observed in pure BPI [25] and DBPI [13]. The main difference with the pure BPI is a maximum of ε'' in the ferroelectric phase. The position of dielectric
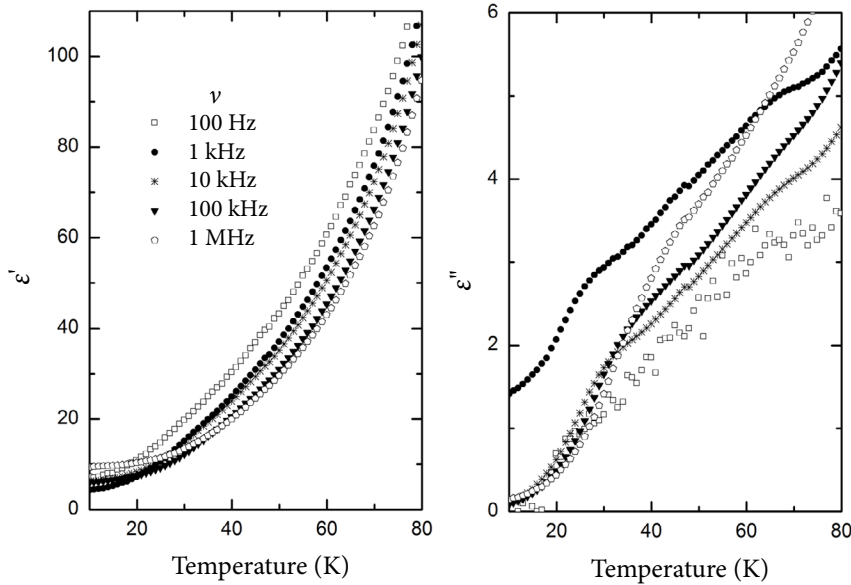
Fig. 7. Temperature dependence of complex dielectric permittivity for $BP_{0.06}BPI_{0.94}$ crystals (low temperature region).

loss maximum is frequency dependent (indicated by an arrow in Fig. 7). This behaviour was described by the Vogel–Fulcher relationship [26]:

$$\nu = \nu_0 e^{-\dfrac{E_t}{k_B(T_m - T_{0t})}}, \tag{17}$$

where T_m is the temperature at which the measured imaginary part of dielectric permittivity ε'' passes through a maximum, ν_0 is the frequency approached with $T_m \rightarrow \infty$; E_t is the activation energy, T_{0t} is the freezing temperature.

The best fit of ν with the Vogel–Fulcher equation is shown as a solid line in Fig. 8. The obtained parameters are $\nu_0 = 2.12$ GHz, $E_t = 293$ K, and $T_0 = 5$ K. The freezing phenomena in betaine phosphite with a small admixture of betaine phosphate reveal the characteristics of a transition into a dipolar glass state: the slowing down of the dipolar degrees of freedom exhibits a broad
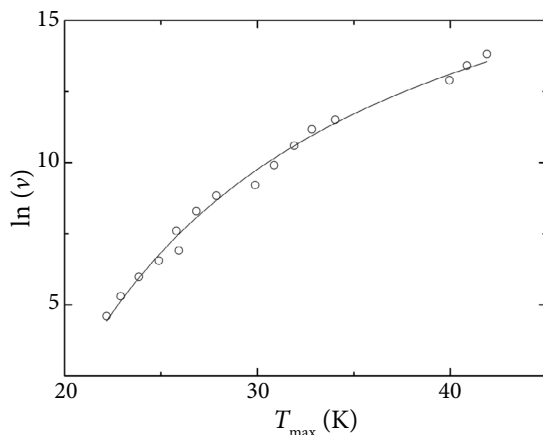
distribution of the relaxation rates, with the width of the distribution exceeding by orders of magnitude the width of a monodispersive Debye process. Similarly to DRADA [27] crystals, $BP_{0.06}BPI_{0.94}$ crystals also exhibit a phase with the coexisting ferroelectric and dipolar glass order at lower temperatures, where part of protons is frozen-in along the one-dimensional chains.

Conclusions

The dielectric properties of mixed $BP_{0.06}BPI_{0.94}$ ferroelectric crystals were investigated in a wide frequency range from 20 Hz to 3 GHz. Although the dielectric anomaly is clearly observed close to the ferroelectric phase transition temperature $T_c = 121$ K, the dielectric dispersion is very broad around and below this temperature. Temperature dependences of the dielectric strength, the mean relaxation frequency and the spontaneous polarization cannot be described together according to the Landau theory for ferroelectric phase transition with a single order parameter or according to the quasi-one-dimensional Ising model. So, $BP_{0.06}BPI_{0.94}$ is not a typical ferroelectric. The local polarization shows a pronounced distribution in the ferroelectric phase and only a partial ordering of hydrogen atoms occurs down to the lowest temperatures. Unordered hydrogen atoms form a glassy phase and its formation is observed in dielectric spectra at very low temperatures. Proton freezing temperature was estimated.

Acknowledgements

Fig. 8. Measurement frequency versus the dielectric loss maximum temperature for $BP_{0.06}BPI_{0.94}$ crystals (low temperature region).

References

[1] R. Ramesh and N.A. Spaldin, Multiferroics: progress and properties in thin films, Nat. Mater. **6**, 21–29 (2007), http://dx.doi.org/10.1038/nmat1805

[2] J. Macutkevic, J. Banys, R. Grigalaitis, and Ju. Vyschanskii, Asymmetric phase diagram of $CuInP_2(S_xSe_{1-x})_6$ crystals, Phys. Rev. B **78**, 064101 (2008), http://dx.doi.org/10.1103/PhysRevB.78.064101

[3] L.E. Cross, Relaxor ferroelectrics, Ferroelectrics **76**, 241–267 (1987), http://dx.doi.org/10.1080/00150198708016945

[4] I. Fehst, M. Paasch, S.L. Hutton, M. Braune, R. Böhmer, A. Loidl, M. Dörfel, Th. Narz, S. Haussühl, and G.J. Mcintyre, Paraelectric and ferroelectric phases of betaine phosphate: structural, thermodynamic, and dielectric properties, Ferroelectrics **138**, 1–10 (1993), http://dx.doi.org/10.1080/00150199308017710

[5] W. Schildkamp and J. Spilker, Structural and antiferroelectric phase transitions in betaine phosphate $(CH_3)_3NCH_2COOH_3PO_4$, Z. Kristalogr. **168**, 159 (1984).

[6] H. Ebert, S. Lanceros-Mendes, G. Schaack, and A. Klöpperpieper, Investigations on dielectric and structural properties of ferroelectric betaine phopshite (BPI), J. Phys. Condens. Matter **7**, 9305–9319 (1995), http://iopscience.iop.org/0953-8984/7/48/019/

[7] M.L. Santos, L.C.R. Andrade, M.M.R. Costa, M.R. Chaves, A. Almeida, A. Klöpperpieper, and J. Albers, Detailed structural X-ray study of betaine phosphate$_{(1-x)}$betaine phosphate$_x$ compounds, Phys. Status Solidi B **199**, 351–367 (1997), http://dx.doi.org/10.1002/1521-3951(199702)199:2<351::AID-PSSB351>3.0.CO;2-D

[8] J. Albers, A. Klöpperpieper, H.J. Rother, and K.H. Ehses, Antiferroelectricity in betaine phosphate, Phys. Status Solidi A **74**, 553–557 (1982), http://dx.doi.org/10.1002/pssa.2210740221

[9] J. Albers, A. Klöpperpieper, H.J. Rother, and S. Hausshühl, Ferroelectricity in betaine phosphate, Ferroelectrics **81**, 27–30 (1988), http://dx.doi.org/10.1080/00150198808008804

[10] H. Bauch, J. Banys, R. Böttcher, A. Pöppl, G. Völkel, C. Klimm, and A. Klöpperpieper, Structural phase transitions in partially deuterated betaine phosphate crystals studied by dielectric and electron paramagnetic resonance methods, Ferroelectrics **163**, 59–68 (1995), http://dx.doi.org/10.1080/00150199508208264

[11] R. Cach, S. Dacko, and Z. Czapla, Dielectric properties of betaine phosphite near ferroelectric phase transition, Phys. Status Solidi A **148**, 585 (1995), http://dx.doi.org/10.1002/pssa.2211480227

[12] R. Sobiestianskas, J. Grigas, Z. Czapla, and S. Dacko, Critical dielectric relaxation in ferroelectric betaine phosphate in the microwave region, Phys. Status Solidi A **136**, 223–228 (1993), http://dx.doi.org/10.1002/pssa.2211360127

[13] G. Fischer, H.J. Brückner, A. Klöpperpieper, H.G. Unruh, and A. Levstik, Dielectric investigations of pseudo one-dimensional betaine phosphate, Z. Phys. B **79**, 301–305 (1990), http://dx.doi.org/10.1007/BF01406599

[14] H. Ries, R. Böhmer, I. Fehst, and A. Loidl, Order parameters and dielectric relaxation in betaine proton glasses, Z. Phys. B **99**, 401–411 (1996), http://dx.doi.org/10.1007/s002570050055

[15] J. Banys, C. Klimm, G. Völkel, H. Bauch, and A. Klöpperpieper, Proton-glass behaviour in a solid-solution of betaine phosphate, Phys. Rev. B **50**, 16751–16753 (1994), http://iopscience.iop.org/0953-8984/8/16/001

[16] M.L. Santos, M.R. Chaves, A. Almeida, A. Klöpperpieper, H.E. Muser, and J. Albers, Dielectric and pyroelectric behaviour in BPI_xBP_{1-x}, Ferroelectrics Lett. **15**, 17 (1993), http://dx.doi.org/10.1080/07315179308203356

[17] J. Banys, P.J. Kundrotas, C. Klimm, A. Klöpperpieper, and G. Völkel, Proton-glass behaviour in a solid-solution of betaine phosphate$_{0.15}$betaine phosphite$_{0.85}$, Phys. Rev. B **61**, 3159 (2000), http://iopscience.iop.org/0953-8984/8/16/001

[18] A. Bussmann-Holder and K.H. Michel, Bond geometry and phase transition mechanism of H-bonded ferroelectrics, Phys. Rev. Lett. **80**, 2173 (1998), http://dx.doi.org/10.1103/PhysRevLett.80.2173

[19] J. Banys, P.J. Kundrotas, C. Klimm, A. Kopperpieper, and G. Volkel, Phase diagram of the mixed crystals betaine phosphate and betaine phosphite: experimental and Monte Carlo results, Phys. Rev. B **61**, 3159–3162 (2000), http://dx.doi.org/10.1103/PhysRevB.61.3159

[20] J. Banys, R. Sobiestianskas, C. Klimm, and G. Völkel, Ferroelectric properties of deuterated betaine phosphite near the ferroelectric phase transition, Lith. J. Phys. **37**, 505 (1997), http://www.itpa.lt/LFD/Lfz/LFZ.html

[21] J. Banys, C. Klimm, G. Völkel, A. Kajokas, A. Brilingas, and J. Grigas, Dielectric investigations of proton glass behaviour in a solid solution of deuterated betaine phosphate$_{0.01}$ betaine phosphate$_{0.99}$, J. Phys. Condens. Matter **13**, 1773 (2001), http://iopscience.iop.org/0953-8984/10/37/023

[22] J. Dolinsek, D. Acron, B. Zalar, R. Pirc, R. Blinc, and R. Kind, Quantum effects in the dynamics of proton glasses, Phys. Rev. B **54**, R6811 (1996), http://dx.doi.org/10.1103/PhysRevB.54.R6811

[23] R. Pirc, B. Tadic, and R. Blinc, Random-field smearing of the proton-glass transition, Phys. Rev. B **36**, 8607 (1987), http://dx.doi.org/10.1103/PhysRevB.36.8607

[24] R. Blinc, J. Dolinsek, A. Gregorovic, B. Zalar, C. Flipic, Z. Kutnjak, A. Levstik, and R. Pirc, Local

polarization distributions and Edwards–Anderson order parameter of relaxor ferroelectrics, Phys. Rev. Lett. **83**, 424 (1999), http://dx.doi.org/10.1103/PhysRevLett.83.424

[25] H. Bauch, J. Banys, R. Böttcher, C. Klimm, A. Klöpperpieper, and G. Völkel, Anomalies of the low frequency dielectric dispersion in betaine phosphate, Phys. Status Solidi B **187**, K81–K84 (1995), http://dx.doi.org/10.1002/pssb.2221870258

[26] G.S. Vulcher, Analysis of recent measurements of the viscosity of glasses, J. Am. Ceram. Soc. **8**, 339–355 (1925), http://dx.doi.org/10.1111/j.1151-2916.1925.tb16731.x

[27] Z. Trybula, V.H. Schmidt, and J.E. Drumheller, Coexistence of proton-glass and ferroelectric order in $Rb_{1-x}(NH_4)_xH_2AsO_4$, Phys. Rev. B **43**, 1287R–1289R (1991), http://dx.doi.org/10.1103/PhysRevB.43.1287

TARPINĖ FAZĖ TARP FEROELEKTRIKAMS BŪDINGOS TVARKOS IR DIPOLINIAMS STIKLAMS BŪDINGOS NETVARKOS MIŠRIUOSE BETAINO FOSFATO$_{0,06}$ BETAINO FOSFITO$_{0,94}$ KRISTALUOSE

J. Banys [a], J. Macutkevic [b], C. Klimm [c], G. Völkel [c]

[a] *Vilniaus universitetas, Vilnius, Lietuva*
[b] *Fizinių ir technologijos mokslų centras, Vilnius, Lietuva*
[c] *Leipcigo universiteto Fizikos ir žemės mokslų fakultetas, Leipcigas, Vokietija*

Santrauka

Straipsnyje pateikti betaino fosfato$_{0,06}$ betaino fosfito$_{0,94}$ plačiajuosčių dielektrinių tyrimų rezultatai. Nors feroelektrinio fazinio virsmo aplinkoje yra stebima dielektrinė anomalija, ji negali būti aprašyta klasikinių feroelektrikams būdingų dėsnių pagalba. Feroelektrinėje fazėje dielektrinė dispersija yra labai plati ir asimetriška. Apskaičiuotas Cole–Cole relaksacijos trukmių pasiskirstymo parametras didėja mažėjant temperatūrai ir žemose temperatūrose pasiekia labai didelę (feroelektrikams) 0,3 vertę. Pasinaudojus dielektriniais spektrais, nustatyti šių kristalų relaksacijos trukmių pasiskirstymai. Šie platūs ir asimetriški pasiskirstymai iš esmės skiriasi nuo siaurų pasiskirstymų, dažniausiai stebimų feroelektrikuose. Pasiskirstymai buvo nagrinėjami pagal dvigubo minimumo potencialo modelį. Iš pasiskirstymų nustatyti dvigubo minimumo potencialo parametrai: potencialinio barjero aukščio vidurkis ir dispersija; potencialinio barjero asimetrijos vidurkis ir dispersija. Pasinaudojus šiais parametrais, apskaičiuoti lokalinės poliarizacijos pasiskirstymai ir vidutinė (makroskopinė) poliarizacija. Gautos makroskopinės poliarizacijos vertės gerai sutampa su eksperimentiškai nustatytomis vertėmis. Šie rezultatai rodo, kad net žemose temperatūrose feroelektrinėje fazėje dalis protonų lieka nesusitvarkę, jie toliau mažėjant temperatūrai sudaro stiklo fazę. Šios fazės susidarymas yra stebimas dielektriniuose spektruose labai žemose temperatūrose. Iš žematemperatūrinių dielektrinių spektrų pavyko nustatyti protonų užšalimo temperatūras.